DEVELOPMENT OF AN ELECTRODEPOSITION PROCESS FOR THE FABRICATION OF A SPHERICAL CRYOGENIC FLUID STORAGE CONTAINER

Prepared for
National Aeronautics and Space Administration
George C. Marshall Space Flight Center
Huntsville, Alabama
Attention: Mr. G. B. Armstrong, PR-ES

Contract NAS8-20094

EOS Report 6951-Final 30 June 1966

Prepared by
R. N. Hanson

Approved by

M. A. Pichel, Manager
Replication and Electroforming Department

ELECTRO-OPTICAL SYSTEMS, INC., — PASADENA, CALIFORNIA
A Subsidiary of Xerox Corporation

FOREWORD

This program was conducted by the Replication and Electroforming Department of Electro-Optical Systems, Inc., Pasadena, California. The work was performed for the NASA George C. Marshall Space Flight Center under Contract NAS8-20094 under the technical direction of Mr. B. K. Davis.

Major contributors to this project were: R. Hanson and J. Tyler, Engineering; G. Hegemier, Stress Analysis; D. DuPree, Electroforming; and L. Amick, Laboratory work.

SUMMARY

32136

A 51-inch-diameter, electrodeposited nickel, spherical pressure vessel was successfully designed, fabricated and tested. The results of this manufacturing process development study have proven the feasibility of fabricating seamless pressure vessels by the electrodeposition process.

The vessel produced was fabricated by depositing nickel on an aluminum mandrel in a nickel sulfamate electroforming bath. The aluminum mandrel was removed after completion of the electroforming process by chemical etching with dilute hydrochloric acid.

A hydrostatic proof test and helium leak test have shown the vessel meets the following design requirements:

Operating Pressure	50 psig
Proof Pressure	70 psig
Helium Permeability	less than 10^{-6} std/cc/sec/ft^2

CONTENTS

1.	INTRODUCTION	1
2.	TECHNICAL DISCUSSION	3
	2.1 Phase I — Design	3
	2.1.1 Vessel Design	4
	2.1.2 Mandrel Design	6
	2.1.3 Current Distribution	9
	2.1.4 Bath Agitation	13
	2.1.5 Bath Chemical Composition	13
	2.1.6 Plating Parameters	13
	2.2 Phase II — Fabrication	14
	2.2.1 Electroforming Mandrel	14
	2.2.2 Electroforming	16
	2.2.3 Mandrel Removal	18
	2.2.4 Thickness Profile	19
	2.2.5 Final Assembly	19
	2.3 Phase III — Testing	22
	2.3.1 Tensile Testing	22
	2.3.2 Hydrostatic Proof Test	22
	2.3.3 Helium Leak Test	24
3.	CONCLUSIONS AND RECOMMENDATIONS	25
	APPENDIX A — ELECTRO-OPTICAL SYSTEMS CRYOGENIC TANK ANALYSIS	A-1
	APPENDIX B — DERIVATION OF ANODE PACK DESIGN EQUATION	B-1

ILLUSTRATIONS

1	51-Inch Diameter Spherical Tank	5
2	51-Inch Diameter Tank Assembly	7
3	Plating Mandrel — 51-Inch Diameter Sphere	8
4	Electroforming Setup — 51-Inch Diameter Nickel Sphere	10
5	Shaped Nickel Anodes on Neck Anode Basket	12
6	Completed Mandrel	15
7	Electroformed Nickel Sphere	15
8	Thickness Profile Final Vessel, 51-Inch Diameter Electroformed Nickel Sphere	20
9	51-Inch Diameter Sphere Showing Fill Value	21
10	51-Inch Diameter Sphere Showing Drain and Relief Value	21
11	Hydrostatic Proof Test — Pressure Versus Time 51-Inch Diameter Nickel Sphere	23
12	Variation of Nickel Properties as a Function of Bath Temperature	27

1. INTRODUCTION

The purpose of this process development program was to design, fabricate and test a 51-inch-diameter, electroformed nickel, spherical cryogenic fluid container.

Conventional cryogenic containers are fabricated from austenitic-type steels with a face-centered cubic lattice structure. This lattice structure is not subject to the brittle transition at cryogenic temperatures noted with materials having the body-centered cubic space lattice. Difficulties encountered with these vessels usually arise at the joints where end closures are welded or where port openings and reinforcements are joined. Development studies with composite chambers fabricated from glass fibers and epoxy resins have indicated that these chambers have high strength-to-weight ratios, but have also pointed out extremely serious problems of permeability, (elastomeric liners cannot be used at cryogenic temperatures), and low stiffness of the composite matrix. When metallic foil liners are used to prevent permeability, the composite overwrap must be overdesigned to insure strain compatibility between the liner and shell. Otherwise, the cycle fatigue life will be greatly reduced because the liner will be strained into the plastic range.

The electroforming process offers a solution to the problem of welds and liners as a continuous joint-free structure can be produced. Changes in thickness of the vessel wall can be made to reinforce local high-load areas, eliminating the need of extensive machining and welding after the vessel is formed. Major problems with the electroformed structure are insuring a "pin hole" free vessel and establishing the proper design and fabrication parameters. Since only a limited amount of development data have been reported in this area, the program had

three main areas of effort: Phase I - design of a vessel suitable for the electroforming process and definition of the process to be used to fabricate the vessel; Phase II - fabrication of a 51-inch-diameter spherical pressure vessel to verify the design and process procedures developed under Phase I; and Phase III - testing of the fabricated vessel to verify that design and process requirements had been met.

2. TECHNICAL DISCUSSION

2.1 Phase I - Design

Nickel electroforming is defined as the "production or reproduction of articles by electrodeposition upon a mandrel or mold that is subsequently separated from the deposit".

Electroforming is accomplished by placing the mandrel or article that is to be electroformed in an electrolyte solution. Nickel anodes are placed in the electrolyte in an arrangement that will produce the desired metal distribution over the mandrel. A direct current is passed between the nickel anodes and the mandrel which functions as the cathode. The electric current frees nickel cations at the anode, which then recombine as elemental nickel at the cathode. The electric current is maintained until the desired wall thickness of nickel has been produced.

Several parameters which affect the electroforming process must be carefully considered. These parameters are:

1. Part Design
2. Mandrel Design
3. Current Distribution
4. Bath Agitation
5. Bath Chemical Composition
6. Plating Parameters
    a. pH
    b. Temperature
    c. Current Density
    d. Plating Stress

2.1.1 Vessel Design

Design loads and compatibility of the vessel with the electroforming process were the primary factors considered in the vessel design.

A spherical shape was selected because the primary structural load was from the internal pressure. Electroformed nickel is an isotropic material and the spherical shape gives the largest volume vessel for a minimum surface area and thickness.

Processing mandrel size and axial symmetry considerations required that the vessel be rotated during the electroforming process. The current distribution varies somewhat from point to point in the electroforming bath. Since the thickness of the deposited material is directly related to the current density, rotation of the mandrel was necessary to minimize variations in thickness. As a result of the rotation requirement, the fill and drain openings were located symmetrically to simplify anode and masking designs. The final vessel design is shown in Fig. 1.

The maximum stresses expected during proof testing were established by using the structural analysis presented in Appendix A. This analysis defines the expected thermal and pressure stresses for a 51-inch-diameter spherical pressure vessel as a function of wall thickness. The analysis indicates that the maximum pressure stress can be expected at the junction of the port opening and the shell. The stress in this area is approximately 2.5 times the stress predicted by membrane theory. The vessel is 0.060-inch thick in this area, giving a membrane stress of 15,000 psi as shown in Fig. A-2. Based on the stress concentration factor of 2.5, the maximum stress at the discontinuity is 37,500 psi. Temperature induced stresses arise from two sources: temperature gradients along the wall of the vessel and temperature gradients through the wall of the vessel. The maximum thermal stress along the wall is 40,000 psi as shown in Fig. A-5; the maximum

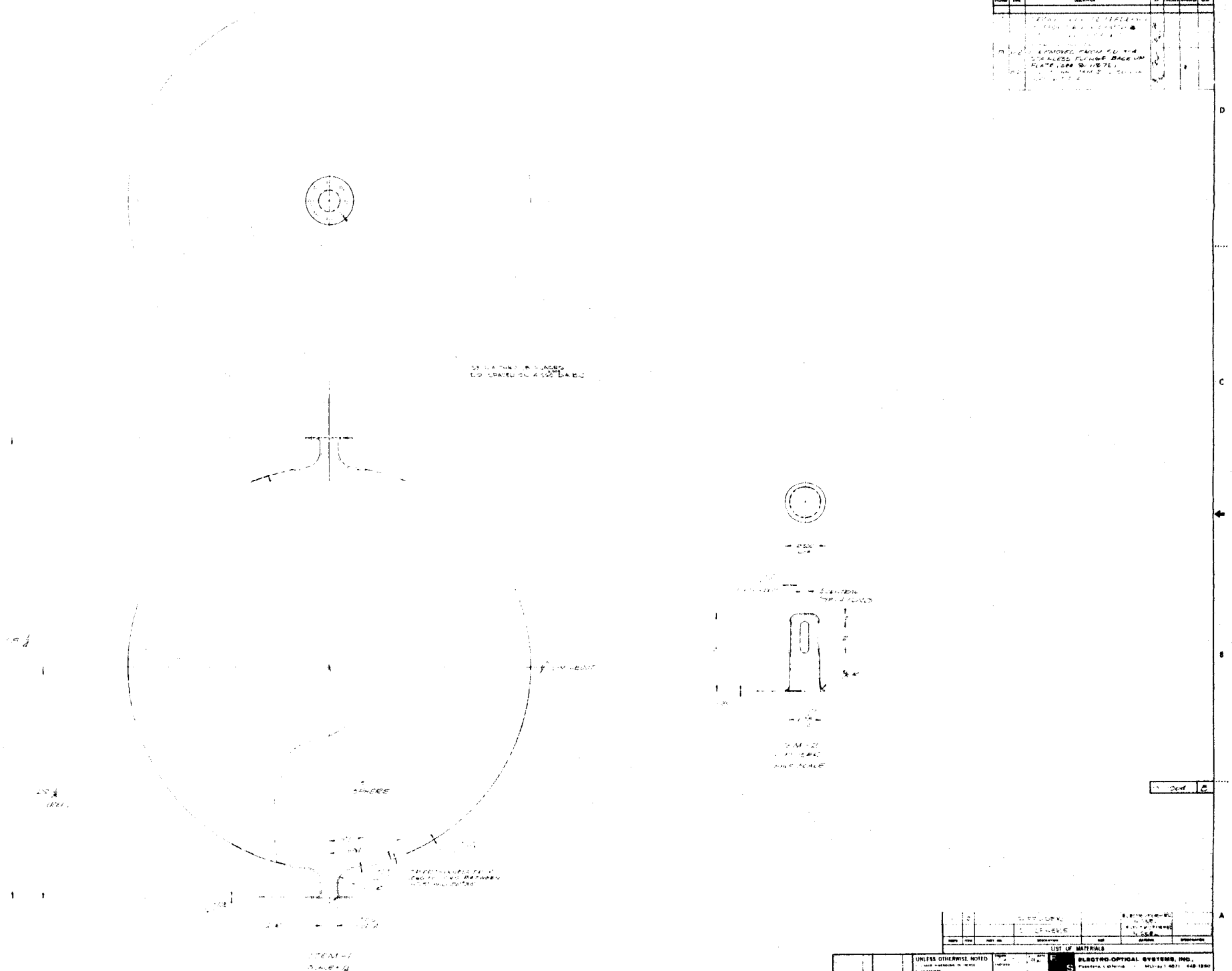

FIG. 1 51-INCH DIAMETER SPHERICAL TANK

temperature stress through the wall is shown to be 53,700 psi. Normally the total stress would be equal to the summation of membrane stress and thermal stress; however, in this case these stresses are a function of the filling rate, and the maximums will not occur simultaneously.

The maximum pressure stress cannot be developed until the vessel is nearly full of liquid; at that time the wall temperature of the vessel should be fairly uniform and the temperature induced stresses minimized.

The membrane stress in the major portion of the vessel at proof pressure will be 22,500 psi. This stress level is extremely low for nickel and a thinner wall thickness could have been used. The 0.040-inch wall thickness was preferred, however, because of the handling and testing risks involved with a first-article vessel.

The sealing and valve mounting arrangements for the pressure vessel during testing are shown in Fig. 2. The nickel flange is supported between two stainless steel plates having sufficient stiffness to develop the full sealing pressures required for cryogenic applications.

2.1.2 Mandrel Design

Mandrels used in the electroforming process are generally classified as permanent or expendable. The distinction is not based upon the material from which the mandrel is made but rather on the manner in which it is used. The requirement that the mandrel must be removed after the electroforming process through two relatively small openings precluded the use of a permanent mandrel in this case. Therefore, an expendable mandrel was selected which could be removed by etching with dilute hydrochloric acid after the electroforming process was completed. The mandrel was made of 6061 aluminum, a material which could be removed without damaging the nickel vessel. The mandrel design is shown in Fig. 3.

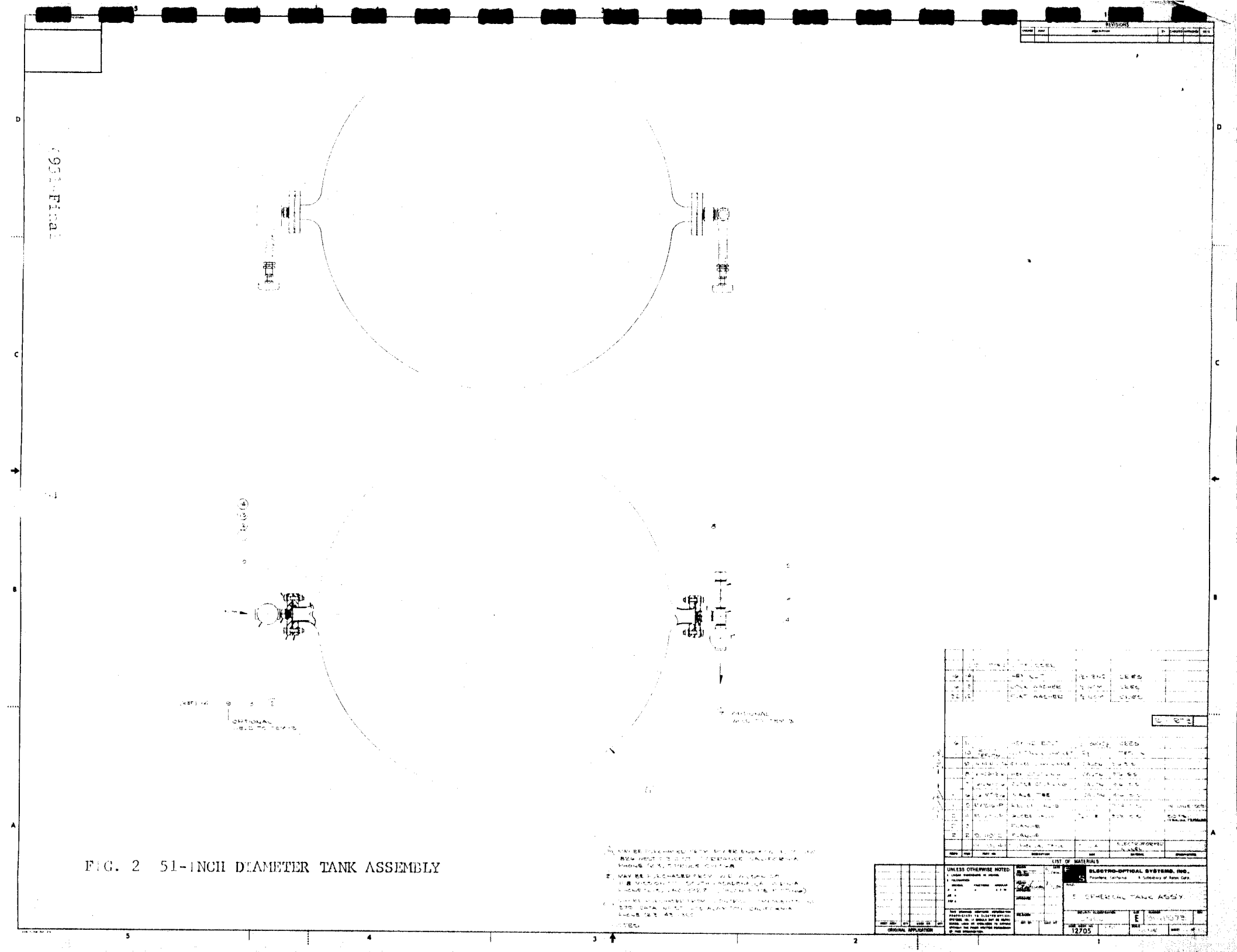

FIG. 2 51-INCH DIAMETER TANK ASSEMBLY

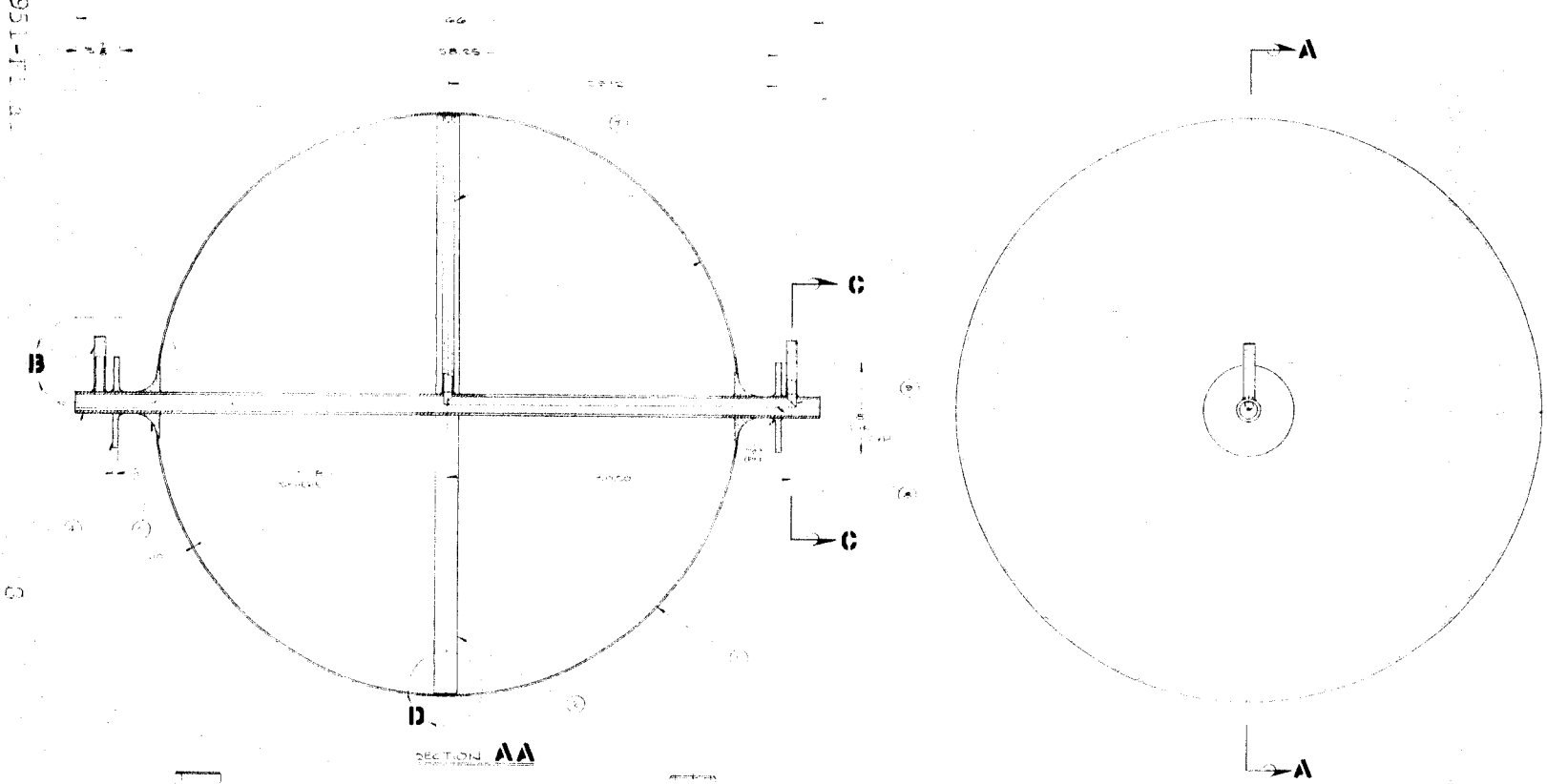

SECTION AA

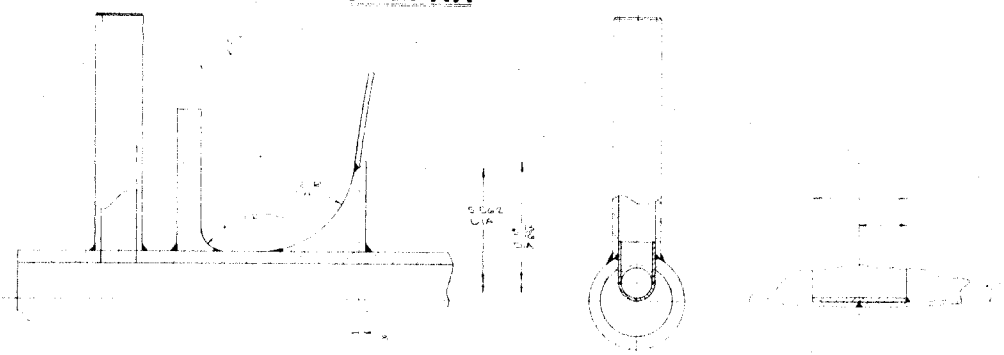

FIG. 3 PLATING MANDREL — 5½-INCH DIAMETER SPHERE

2.1.3 Current Distribution

Current distribution in the electroforming bath is a function of the plating bath geometry, the masking, and anode placement arrangements. The proper combination of these parameters was established from a combined analytical and empirical study. A cross-sectional view of the plating tank setup is shown in Fig. 4. The mandrel is mounted horizontally in the rotating fixture and rotates about a shaft through the center of the mandrel. The vessel is located in the electroforming bath with the center shaft at the surface of the sulfamate plating solution. The main anode pack is suspended beneath the vessel from the horizontal rotator. (The anode pack contains the supply of nickel plating anodes.)

A uniform thickness over the major area of the vessel was obtained by maintaining the ratio of mandrel surface area to anode pack surface area constant at every point, while keeping a constant distance between the mandrel surface and anode pack. The equation below (developed in Appendix B) was used to establish the width of the anode pack at any point,

$$W_\theta = \frac{2\pi R^2 \cos\theta}{(R + h)\, K}$$

where

W_θ = width of anode basket at angle θ, in inches
h = distance between mandrel and anode basket, in inches
R = radius of mandrel in inches
K = ratio of anode basket surface area to mandrel surface area.

The width of the anode basket was established using, h = 8 inches, K = 8 and R = 25.5 inches. It varied from a maximum of 15 inches at the bottom of the mandrel ($\theta = 0^o$), to a minimum of 4.5 inches just below the neck of the vessel ($\theta = 72^o$).

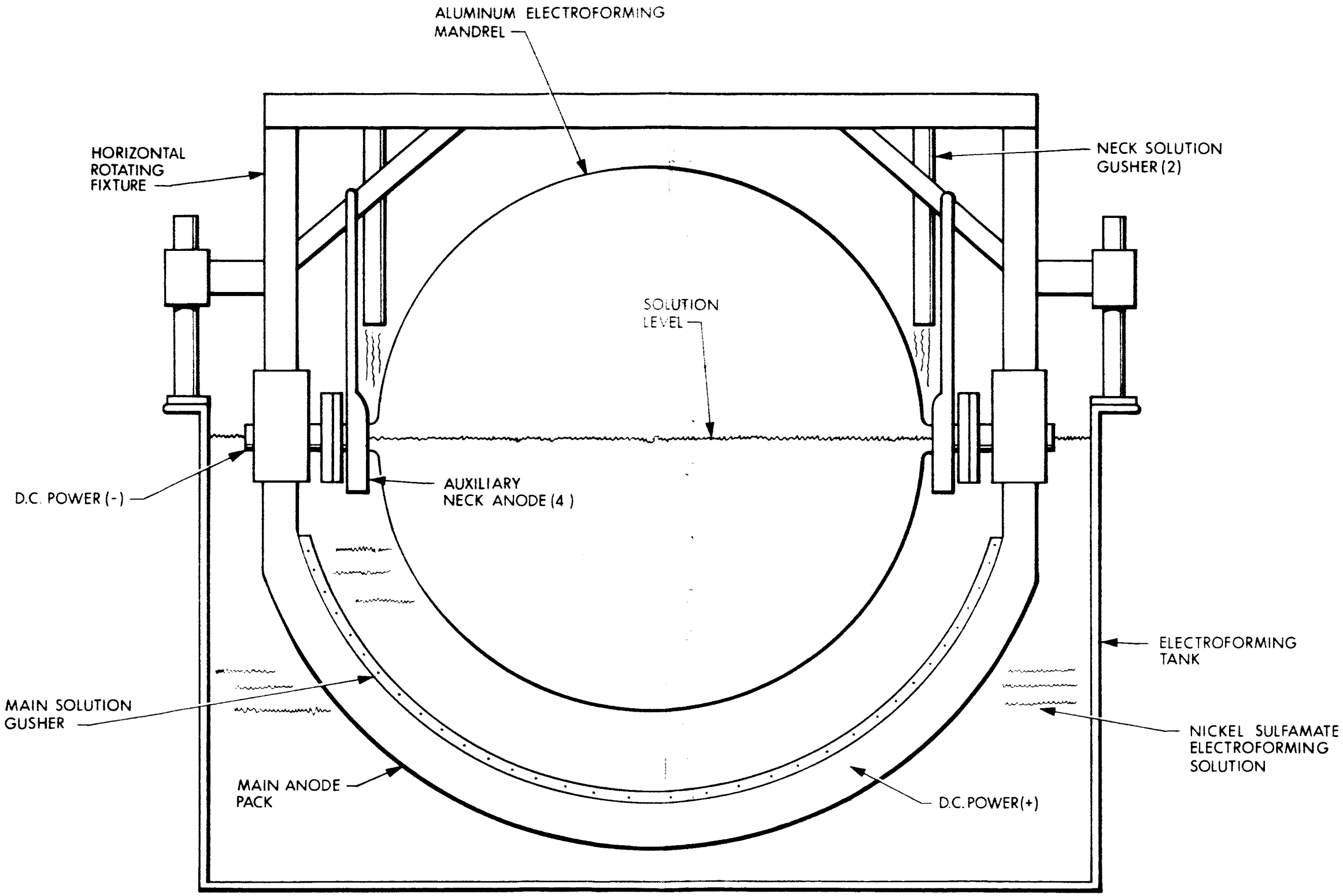

FIG. 4 ELECTROFORMING SET-UP - 24-INCH DIAMETER NICKEL SPHERE

10-1

The additional nickel thickness required in the neck areas to reduce the discontinuity stresses was obtained by using additional auxiliary anodes in the neck area as shown in Fig. 4. These additional anode baskets were controlled on separate direct current rectifiers so that the thickness in this area could be controlled independently of the rest of the vessel surface.

To verify the design concepts of the plating bath geometry, several thickness profiles were made to establish the cross section of the electroformed deposit. These profiles were electroformed by taping off gore sections on the main part of the mandrel so that the electroformed sections could be removed after the plating process without damage to the mandrel. The gore sections were then inspected for thickness variations throughout the profile. During these profile studies it was established that the thickness of the electroformed nickel could be measured during the electroforming process by using a Vidi-gage ultrasonic thickness tester. The profile studies verified that the desired thickness could be readily obtained over the major portion of the sphere. However, several masking changes were made in the areas of the port openings. This was an area of extreme change in curvature on the surface of the mandrel and the current distribution was somewhat uneven. The major problem area was at the junction of the flange and the neck radius; this area built up at a much slower rate than the surrounding areas. Several masking configurations were attempted but did not provide sufficient nickel build-up on the radius. The situation was finally corrected by mounting four additional single anodes to throw directly into the radius. These anodes were mounted on the auxiliary anode baskets. These small anodes were each run off a separate current rectifier so that the current density could be controlled more accurately. These anodes are shown mounted on the auxiliary neck anodes in Fig. 5.

FIG. 5 SHAPED NICKEL ANODES ON NECK ANODE BASKET

2.1.4 Bath Agitation

Proper agitation of the electroforming bath when fabricating pressure vessels is extremely important. Pitting and pinhole effects can be greatly reduced by obtaining the proper bath agitation for the electroforming process. Agitation was obtained by pumping the plating solution through a spray tube mounted along the edge of the main anode basket. The resulting spray then impinged directly upon the plated surface of the mandrel as the vessel rotated in the plating solution. Agitation in the neck areas was provided by pumping the solution up through piping at the top of the rotator, from where it impinged on an area directly above the neck of the vessel. These bath agitation techniques proved adequate for the electroforming process.

2.1.5 Bath Chemical Composition

The electroforming bath selected was a standard sulfamate nickel plating solution, typical of a bath that would be used when producing any heavy wall electroform. The bath had the following chemical composition:

Nickel	8.31 oz/gal.
Nickel chloride	0.38 oz/gal.
Boric Acid	4.94 oz/gal.

The chemical composition of the electroforming solution was monitored throughout the plating process by daily chemical analysis for the three major constituents of the bath.

2.1.6 Plating Parameters

The physical properties of an electroformed nickel deposit can be varied by changing the plating parameters of the electroforming bath. The most significant parameters are (1) hydrogen ion concentration, (2) bath temperature, (3) current density, and (4) plating stress. Proper combination of these plating parameters can produce nickel with such widely varying properties as an ultimate tensile

strength of 200,000 psi with an elongation of 3 percent, to an ultimate tensile strength of 50,000 psi with an elongation of 15 percent. As the vessel fabricated under this program was designed for a cryogenic environment it was desirable to have an elongation in the wall of at least 10 percent in 2 inches. To establish the proper combination of plating parameters to obtain the 50,000 minimum yield strength and a 10 percent elongation in 2 inches, several tensile panels were plated under varying conditions. The desired physical properties were obtained from a sulfamate bath operating at the following conditions:

pH	3.0 to 3.7
Temperature	100°F
Current Density	20A/sq ft
Plating Strength	5000 to 10,000 psi (tensile)

Each of the plating parameters was monitored throughout the plating process to insure that the deposited nickel would have the required physical properties.

2.2 Phase II - Fabrication

Under Phase II of this program a 51-inch-diameter spherical pressure vessel was electroformed to the design requirements and process specifications developed under the Phase I studies.

2.2.1 Electroforming Mandrel

The mandrel was fabricated by spinning two aluminum hemispheres and welding them together on an aluminum center shaft. During the welding process considerable shrinkage occurred at the weld joint, leaving this area of the vessel below the desired contour. This surface deviation was repaired with an aluminum filled epoxy resin capable of curing at room temperature. The surface was prepared for electroforming by painting the surface with a primer, and then coating with a silver conductive paint. The completed mandrel, ready for electroforming, is shown in Fig. 6. The mandrel is shown on the horizontal rotator with the main anode basket and auxilary neck anodes mounted in place.

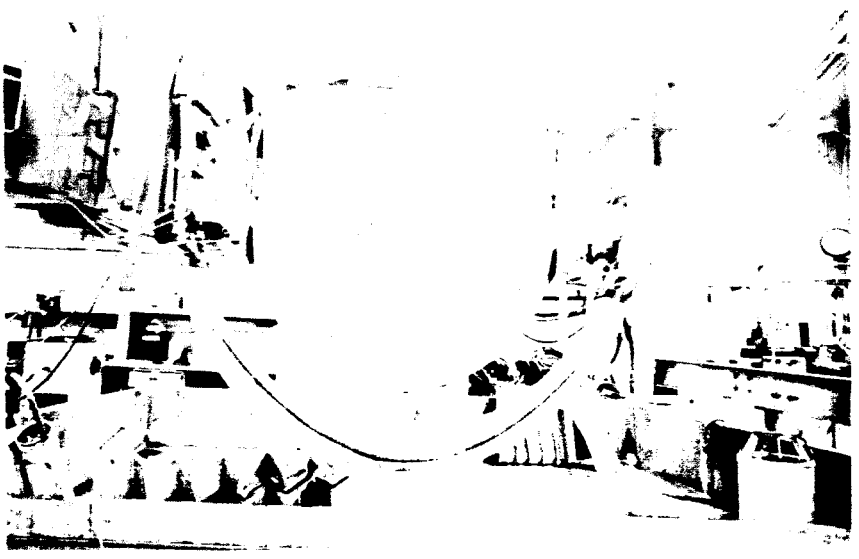

FIG. 6 COMPLETED MANDREL

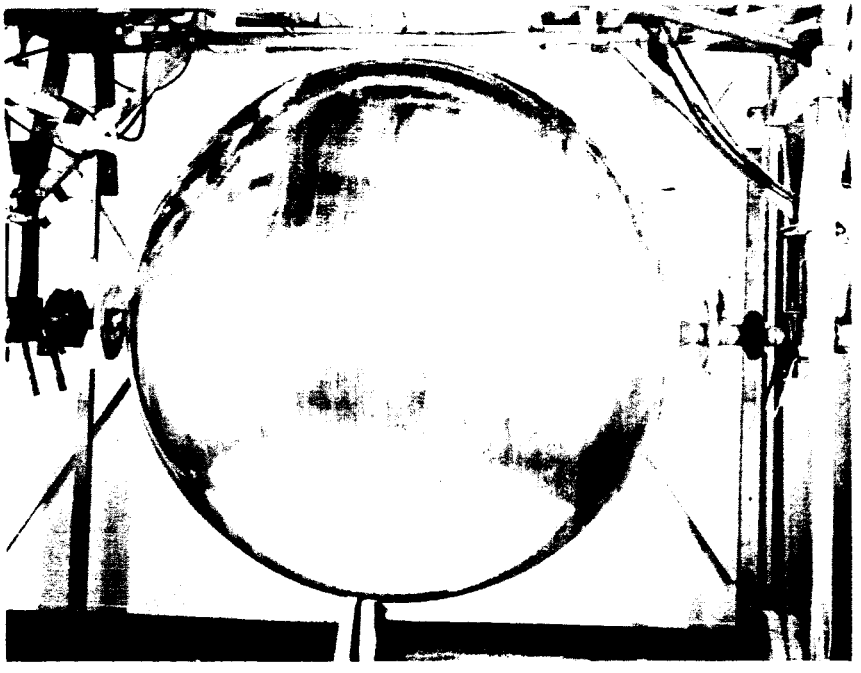

FIG. 7 ELECTROFORMED NICKEL SPHERE

2.2.2 Electroforming

During the electroforming process the mandrel was rotated in the nickel sulfamate bath. The chemical composition of the bath was:

Nickel	8.31 oz/gal.
Nickel Chloride	0.38 oz/gal.
Boric Acid	4.94 oz/gal.

The following plating parameters were maintained throughout the plating process:

pH	3.0 to 3.7
Current density	8 to 10A/sq ft
Bath temperature	100 to 106^{o}F
Plating stress	5000 to 10,000 psi (tensile)

Tensile panels were plated before and after the electroforming of the vessel to establish that the electroposited nickel was meeting the design requirements. Tensile test specimens were prepared from these panels in accordance with ASTM-E8. Test results are presented in Table I. The average properties of these specimens were:

Ultimate tensile strength	81,160 psi
Yield strength (0.2 percent offset)	56,400 psi
Ultimate elongation (2-inch gage length)	13.5 percent
Modulus of elasticity	21.7 x 10^{6} psi

Since the tensile specimens had shown that the nickel deposit was meeting design requirements, the vessel, rotator and anode pack were placed in the electroforming bath. The electroforming process lasted approximately 120 hours. At various times during this period it was noticed that small pits developed on the surface of the nickel. If allowed to continue, the pits might have penetrated the wall of the completed vessel. Therefore, these areas were repaired during the electroforming process. A small local area around the pit was dried and then the pit coated with Du Pont conductive paint number 4929. The conductive paint was dried with a heat gun and plating immediately resumed. This technique appeared to work very well giving a continuous

TABLE I

NICKEL ELECTROFORMED SPHERE TENSILE TEST PANELS
PLATED BEFORE AND AFTER THE VESSEL

Specimen		Ultimate Tensile Strength psi	Yield Strength psi	Elongation in 2 Inches percent	Modulus of Elasticity psi
Before Plating	-1	80,000	54,900	13.0	20.7×10^6
	-2	80,800	61,200	14.0	21.5×10^6
	-3	80,600	55,800	13.0	22.4×10^6
	-4	80,200	54,800	13.5	21.9×10^6
	-5	79,200	55,300	14.0	22.0×10^6
Average		80,160	56,400	13.5	21.7×10^6
After Plating	-1	70,400	45,900	13.0	22.2×10^6
	-2	93,300	64,800	10.5	21.9×10^6
	-3	95,800	68,200	9.0	22.3×10^6
	-4	75,100	49,700	13.5	22.1×10^6
	-5	73,100	47,500	14.0	22.8×10^6
Average		81,540	55,220	12.0	21.8×10^6

nickel layer over the area as soon as electroforming was resumed. The surface was observed continuously throughout the electroforming process and repairs made as soon as possible after a defect was noted.

The electroformed vessel is shown in Fig. 7. Other possible methods of preventing or repairing the surface pitting are (1) burnishing the surface during the electroforming process, and (2) soldering or welding after completion of electroforming. It is believed that pits were started by fine particles of dust which settled on the surface of the plated nickel during the electroforming process. This problem could be completely eliminated on a production basis by electroforming in a clean room or by submerging the entire surface of the vessel in the plating solution.

After electroforming the vessel was sanded to a light polish with 180 grit paper to smooth the surface and improve appearance. Visual inspection of the surface revealed a few small surface pits; the integrity of the shell was verified, however, in later proof and helium test operations.

A second tensile panel was plated after electroforming of the vessel to verify that the electroforming bath was still depositing nickel which met the design requirements. The average physical properties obtained from specimens cut from this panel were:

Ultimate tensile strength	81,540 psi
Yield strength (0.2 percent offset)	55,220 psi
Elongation (2-inch gage length)	12 percent
Modulus of elasticity	21.8×10^6 psi

Test results for each specimen are presented in Table I.

2.2.3 Mandrel Removal

Removal of the aluminum mandrel after electroforming was accomplished by etching in a hydrochloric acid solution (15 percent HCL by volume). Reaction rate was controlled by varying the depth of the vessel in the etching solution. After the aluminum was completely

removed, the epoxy primer and conductive paint, used to repair the contour, were removed by rotating the vessel horizontally with a mixture of fine gravel and high-strength paint remover on the inside. The entire vessel was then rinsed several times with distilled water.

2.2.4 Thickness Profile

The thickness profile was established after the mandrel was removed by using a Vidi-gage ultrasonic thickness tester. The Vidi-gage was calibrated using samples of electroformed nickel of known thickness. The resulting thickness profile is shown in Fig. 8.

The wall thickness of the vessel proper varied between 0.044 and 0.052 inch. The taper necessary to produce the reinforced area started in the proper area and built up to 0.095 inch, 0.020 inch above the expected maximum of 0.075 inch. The reinforced area was covered by the neck auxiliary anode baskets which made it very difficult to obtain Vidi-gage readings during the plating process. Consequently, plating was permitted to continue longer than required to assure an adequate thickness in this high stress area.

The radius between the flange and the neck was thinner than the surrounding areas but should be of adequate thickness for the prototype vessel. The 0.5-inch radius was difficult to build up, as the nickel tended to distribute itself on either the neck or flange.

2.2.5 Final Assembly

Final assembly of the vessel included mounting the flange supports in place and drilling and trimming the nickel flanges to size. The fill, drain and pressure relief valves were mounted on the outer flanges, using stainless steel pipe fittings wrapped with teflon thread tape. While these joints would not be adequate for high vacuum applications they were satisfactory for the qualification tests performed at EOS. The valves can be mounted and welded as required for subsequent cryogenic testing at MSFC. The completed vessel, ready for qualification testing, is shown in Figs. 9 and 10.

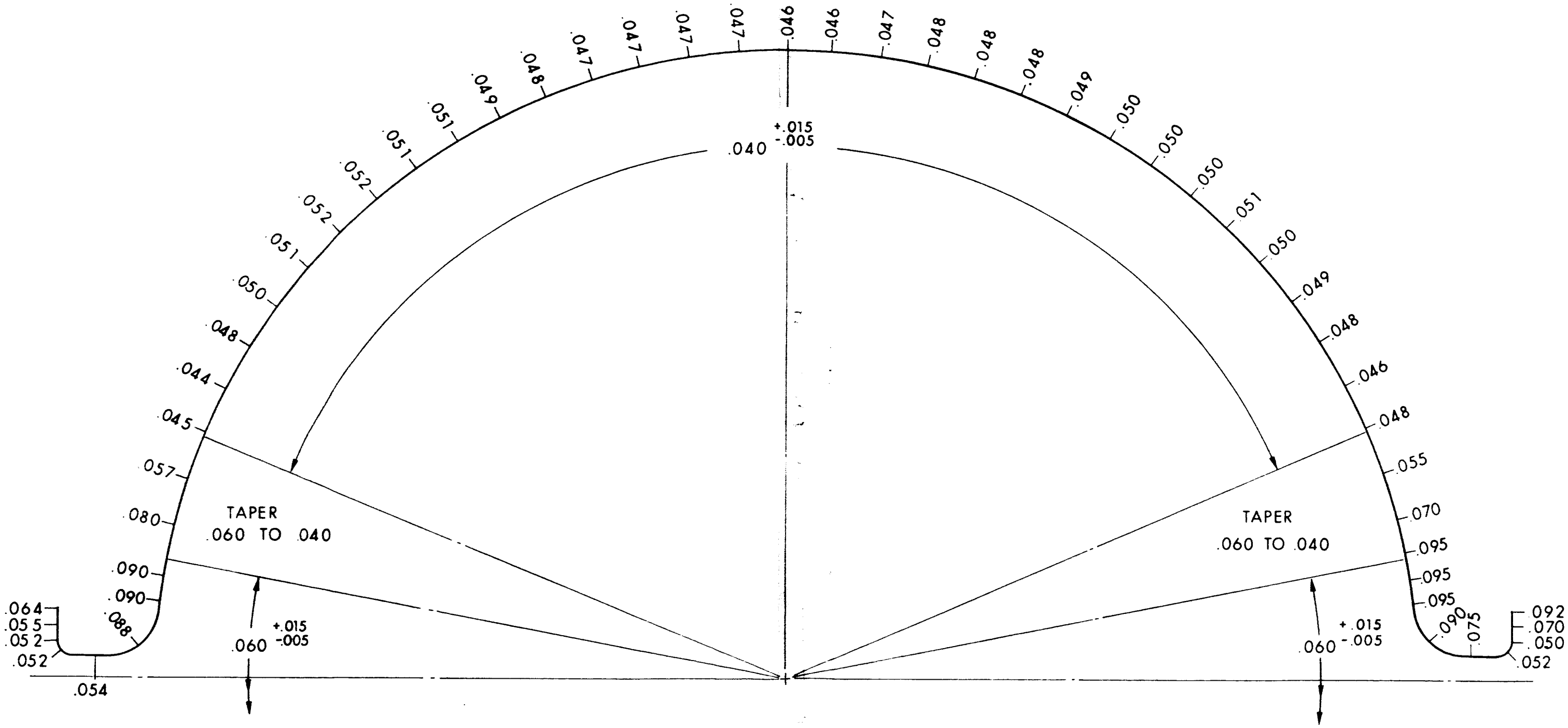

FIG. 8 THICKNESS PROFILE FINAL VESSEL, 2-INCH DIAMETER ELECTROFORMED NICKEL SF ERE

20-1

20-2

6851-Final

736.22257

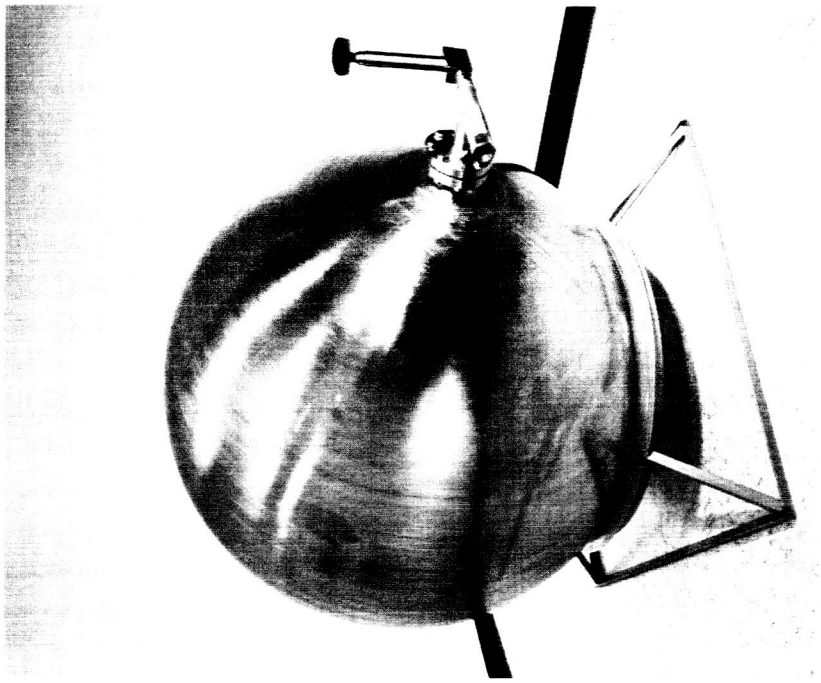

FIG. 9 51-INCH DIAMETER SPHERE SHOWING FILL VALVE

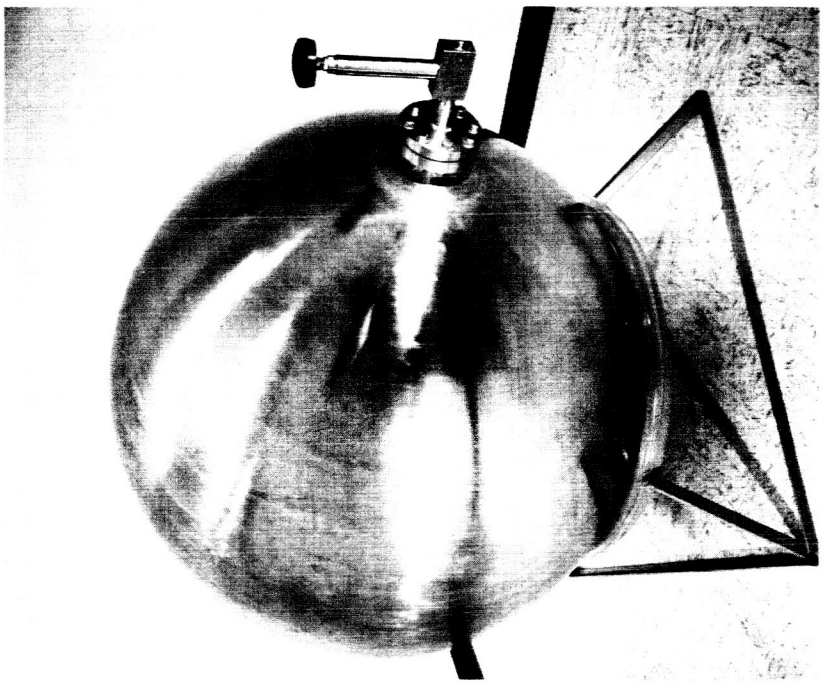

FIG. 10 51-INCH DIAMETER SPHERE SHOWING DRAIN AND RELIEF VALVE

2.3 Phase III - Testing

The purpose of the Phase III testing was to insure that the vessel met the specific design requirements. Testing included (1) tensile testing of specimens to establish mechanical properties attained in the primary structure (2) hydrostatic proof testing of the vessel at 70 psig for 15 minutes and (3) helium leak testing at 15 psig to determine the average permeability rate.

2.3.1 Tensile Testing

The size of the electroformed vessel being fabricated precluded electroforming tensile specimens simultaneously with the vessel during electroforming process. Tensile test panels were therefore plated before and after the vessel was electroformed. The physical properties of the vessel were then assumed to be within the range of those obtained with the test panels.

Five tensile specimens were prepared from each test panel for testing in accordance with ASTM-E8. The specimens were tested in a Riehle tensile testing machine. The design requirements, and the properties of the test panels were as follows:

Property	Design Requirement	Panel Plated Before the Vessel	Panel Plated After the Vessel
Ultimate Tensile Strength (psi)	80,000	80,160	81,450
Yield Strength (2 percent offset) (psi)	50,000	56,400	55,220
Elongation (2-inch gage length) (percent)	10	13.5	12

Specific data from each test are presented in Table I.

2.3.2 Hydrostatic Proof Test

Hydrostatic proof testing was accomplished by assembling the vessel with the flange gaskets, fill and drain fittings, and replacing the pressure release valve with a pressure gage. The vessel was then pressurized with water to 70 psig. The fill and drain valves were closed and pressure maintained for 15 minutes. A pressure versus time curve for this test is shown in Fig. 11. After 15 minutes at

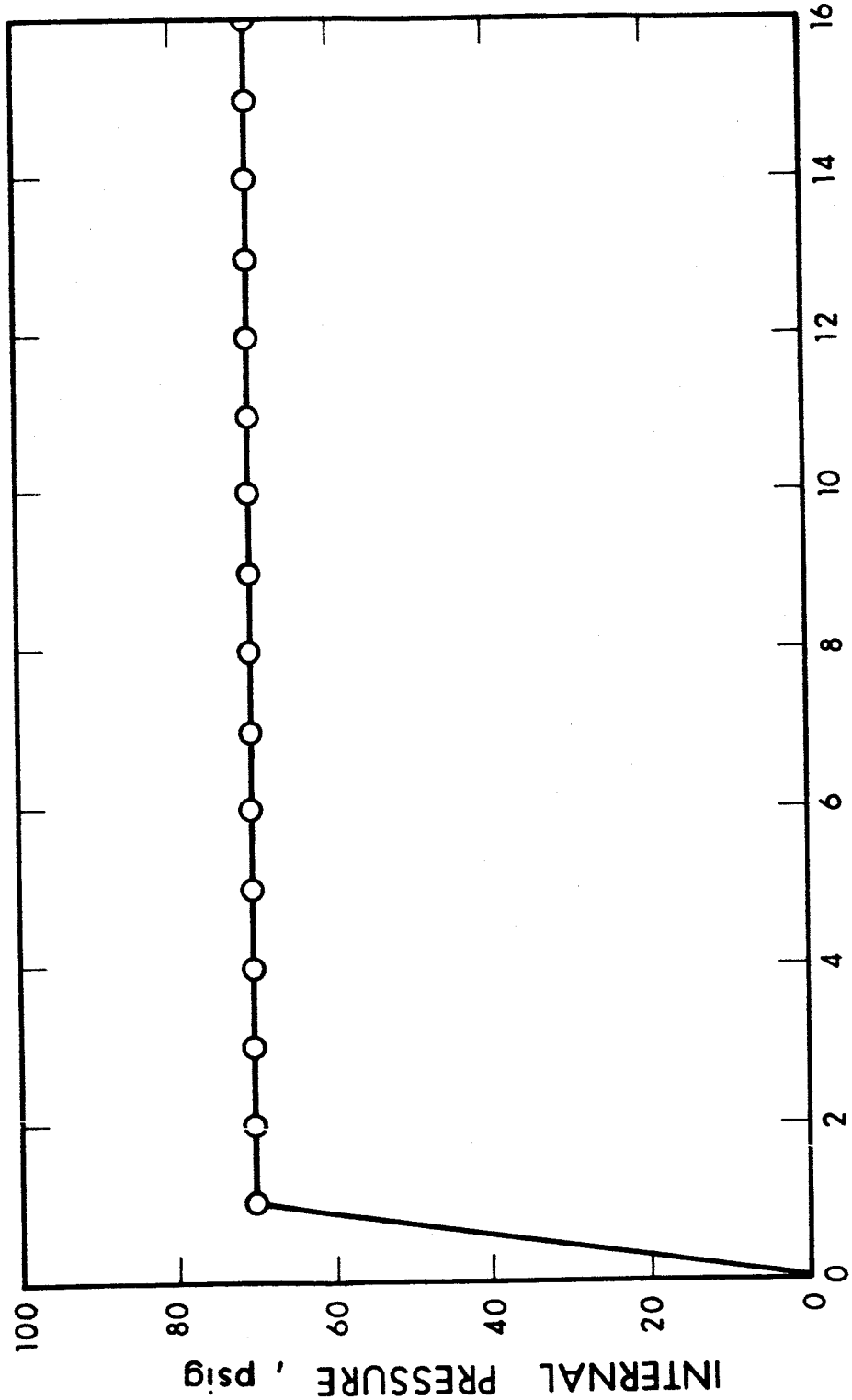

FIG. 11 HYDROSTATIC PROOF TEST – PRESSURE VERSUS TIME 51-INCH DIAMETER NICKEL SPHERE

70 psig there was no drop in pressure, and the vessel was vented. The hydrostatic proof test verified that all components of the vessel could withstand the design proof pressure of 70 psig.

2.3.3 Helium Leak Test

A helium leak test was performed to determine the average permeability rate of the vessel. An initial test was made by pressurizing the vessel internally with helium to 20 psig and then using a helium leak sniffer to establish the leakage rate. The entire surface area was checked and no evidence of a leak was found. The sensitivity of the tester was 1.5×10^{-10} std/cc/sec. The flange seals were also tested; one was leaking at a rate of 6×10^{-6} std/cc/sec and the other at 4.5×10^{-7} std/cc/sec. The Teflon-stainless steel Flexitallic seals used during this test were then replaced with standard rubber flange gaskets. These gaskets sealed the flange area somewhat inside that area which was sealed by the Flexitallic flange gaskets. The entire vessel was then sealed in a polyethylene bag. The helium sniffer was inserted at the top of the bag and the vessel tested for two hours. The maximum leak rate measured during this time was 4.5×10^{-8} std/cc/sec. This rate included the flange seals and the entire surface area of the sphere.

3. CONCLUSIONS AND RECOMMENDATIONS

The feasibility of manufacturing cryogenic pressure vessels by the nickel electroforming process has been successfully demonstrated. A one-piece spherical pressure vessel was designed and fabricated from electrodeposited nickel. The vessel has met design requirements, passed hydrostatic proof test and helium tests for permeability of the vessel wall. The vessel has been delivered to MSFC for further cryogenic testing. Fabrication and testing of the 51-inch-diameter vessel has proven the feasibility of the electroforming process and satisfactorily demonstrated the following:

1. A continuous, nonporous nickel wall can be fabricated.
2. Small pin holes that appear during the electroforming process can be located and successfully repaired during electroforming.
3. The aluminum mandrel can be etched out without damage to the vessel after electroforming has been completed.
4. Changes in wall thickness can be made by proper anode and masking design to provide reinforcement of high load areas, without secondary bonding and welding to the vessel.
5. Port openings and reinforcements can be electroformed simultaneously with the primary structure of the vessel, eliminating a need for secondary welding.
6. The thickness of the electroformed structure can be monitored throughout the plating process with the use of an ultrasonic Vidi-gage thickness tester.

Although it has been shown that pin holes and surface defects can be repaired successfully during electroforming process it would be desirable to eliminate, or at least minimize, the need for such repairs. In several cases it was noticed that the pin holes were started by

specks of dust falling on the surface of the sphere during the plating process. This problem could be solved by either plating in a tank large enough to submerge the entire surface of the sphere in the plating solution or in a clean room atmosphere.

Although the feasibility of electroforming cryogenic pressure vessels has been demonstrated, it is realized that the low tensile strength of the nickel combined with the high density, yields a low strength-to-weight ratio vessel. However, it has been shown during this program that the properties of the electrodeposited nickel can be varied over a large range by proper combination of the plating parameters. An example is shown in Fig. 12, which presents the physical properties of electrodeposited nickel plated in a sulfamate plating bath as a function of the bath temperature. It can be seen that tensile properties were obtained varying from about 100 ksi to 200 ksi and elongations from 3 to 8 percent, depending on the plating temperature. These data indicate that it should be possible, with further study, to produce an electroformed structure that has strength-to-density ratios approximately equal to other common pressure vessel materials; a target value might be 0.6×10^6 inch.

It is recommended that a program be initiated with the objective of evaluating the ultimate tensile strength and elongation of the nickel produced from other nickel plating baths as a function of the plating parameters. This program should also include the electroforming of several smaller size pressure vessels at these plating parameters and the verification of their performance with hydrostatic proof tests.

Such a program would define the proper combination of plating parameters which would result in the production of nickel-deposited pressure vessels capable of performing at levels equal to or better than those currently obtained with vessels produced by more conventional techniques.

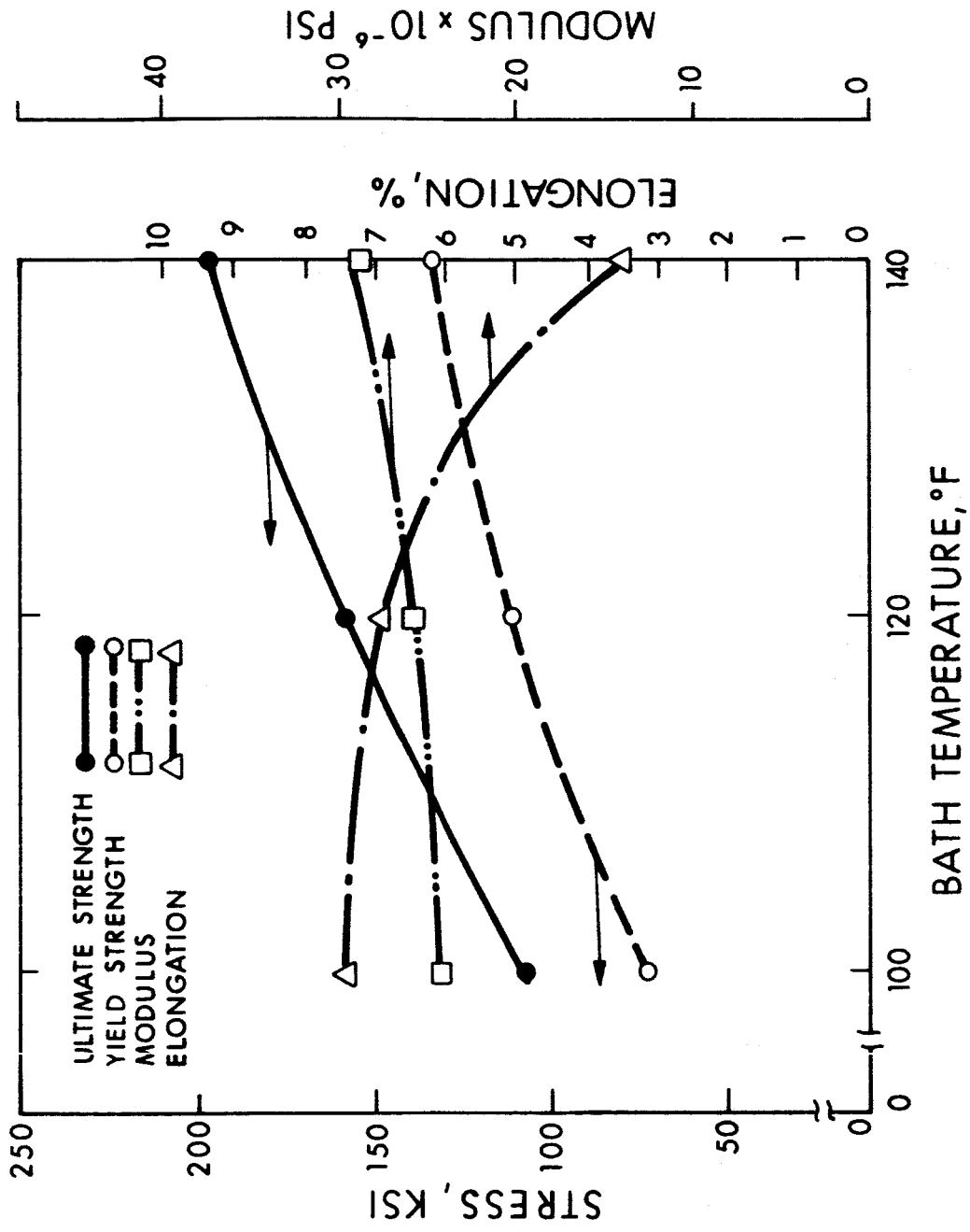

FIG. 12 VARIATION OF NICKEL PROPERTIES AS A FUNCTION OF BATH TEMPERATURE

APPENDIX A

ELECTRO-OPTICAL SYSTEMS CRYOGENIC TANK ANALYSIS

BY G. A. HEGEMIER

1. INTRODUCTION

The information contained herein concerns the stress analysis of the Electro-Optical Systems 51-inch spherical cryogenic storage container. The discussion is restricted to effects of internal pressure and temperature only.

2. GENERAL PROBLEM AREAS

Three basic problem areas should be noted immediately. First, stress concentrations can be expected near the inlet (exhaust) - sphere intercepts. An upper bound on the magnitude of the concentrations will be determined. Second, stress concentrations will exist near the gas-fluid interface when the tank is partially filled with liquid hydrogen. These concentrations are due to the discontinuous nature of the temperature distribution near the interface. And third, there exists the problem of thermal shock; during a short period following contact of the cold liquid with the container wall a rather severe temperature gradient will exist through the wall thickness. This gradient decreases repidly with time and the wall eventually assumes a relatively constant temperature in the thickness direction. However, during the period of large temperature gradient, temperature induced stresses can be large; an estimate of these temperature induced stresses is made.

3. ANALYSIS

Membrane Stress State: Consider Fig. A-1. The stress distribution some distance (to be specified later) away from the flange and gas-fluid interface areas will be that of a pure membrane state. An elementary calculation yields

$$\sigma_m = \sigma_\phi = \sigma_\theta = Pa/2h \qquad (1)$$

where σ_m = membrane stress, σ_ϕ and σ_θ = meridional and hoop stresses, respectively, P = internal pressure, h = shell wall thickness, and a = shell midsurface radius. The behavior of σ_m for P = 70 psi (proof test pressure) and a = 25.5 in. is illustrated in Fig. A-2 for 10×10^{-3} in. $< h < 80 \times 10^{-3}$ in.

Stresses Near the Sphere - Flange Intercept Zone: Reference is again made to Fig. A-1. The magnitude of the stress concentrations near the intercept area for a nonoptimum shell design will be estimated by considering two limiting cases: a connection with zero flexibility (a rigid insert) and a connection with zero rigidity (a hole). Figure A-3 illustrates the rigid insert condition. The stresses in a region $|\phi| < 25^\circ$ can be obtained from Ref. 1 for this case. One finds

$$\frac{\sigma_\phi}{\sigma_m} = 1 + \left\{ (1-\nu)\, \psi_3'(\xi_o) \left(\frac{\psi_3'(\xi)}{\xi} - \frac{3}{\sqrt{3(1-\nu^2)}}\, \psi_3(\xi) + \frac{1-\nu}{\xi}\, \psi_4'(\xi) \right) \right.$$
$$\left. + (1-\nu)\, \psi_4'(\xi_o) \left(\frac{\psi_4'(\xi)}{\xi} - \frac{3}{\sqrt{3(1-\nu^2)}} \left(\psi_4(\xi) - \frac{1-\nu}{\xi}\, \psi_3'(\xi) \right) \right) \right\} \qquad (2)$$
$$\left[\psi_3(\xi_o)\, \psi_4'(\xi_o) - \psi_4(\xi_o)\, \psi_3'(\xi_o) + \frac{1-\nu}{\xi_o} \left(\psi_3'^2(\xi_o) + \psi_4'(\xi_o) \right) \right]^{-1}$$

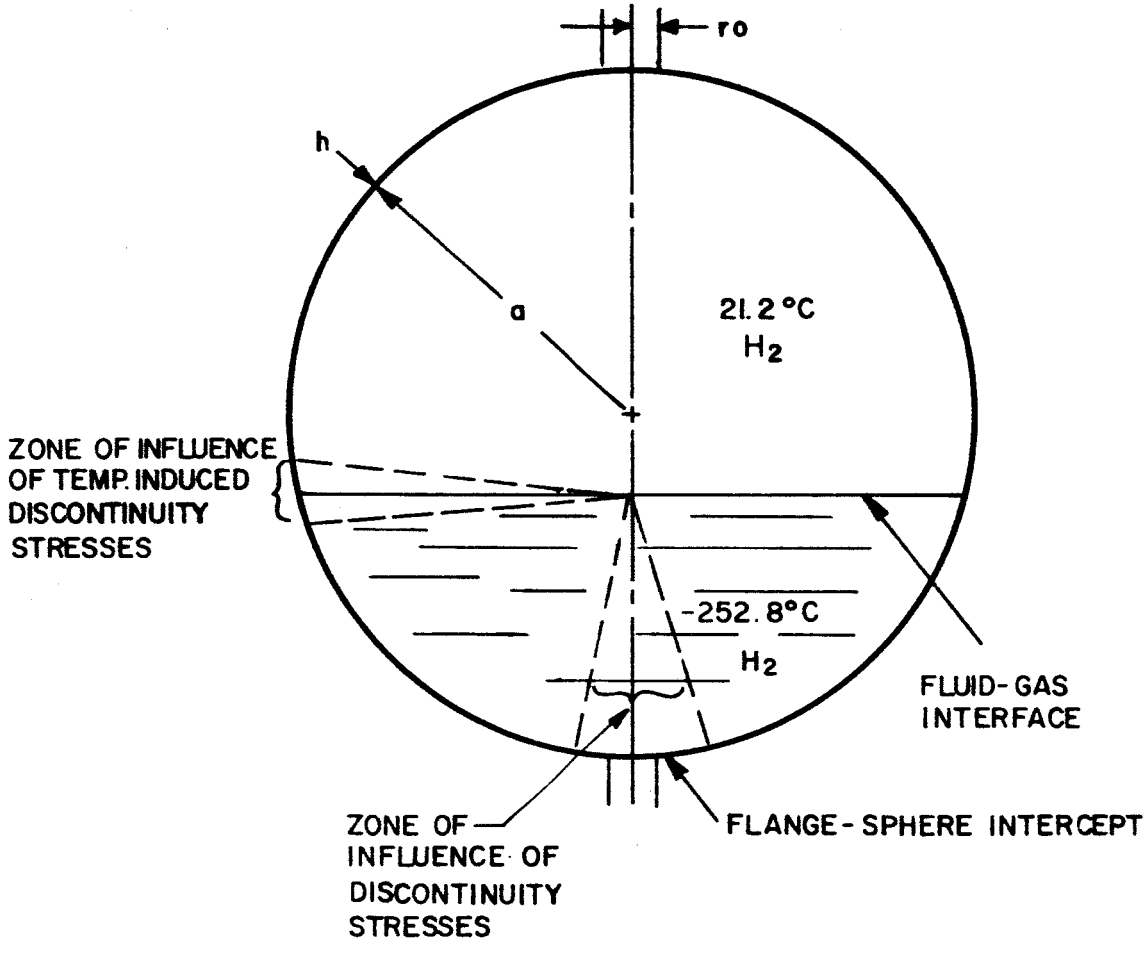

FIG. A-1 THERMAL STRESS FACTORS

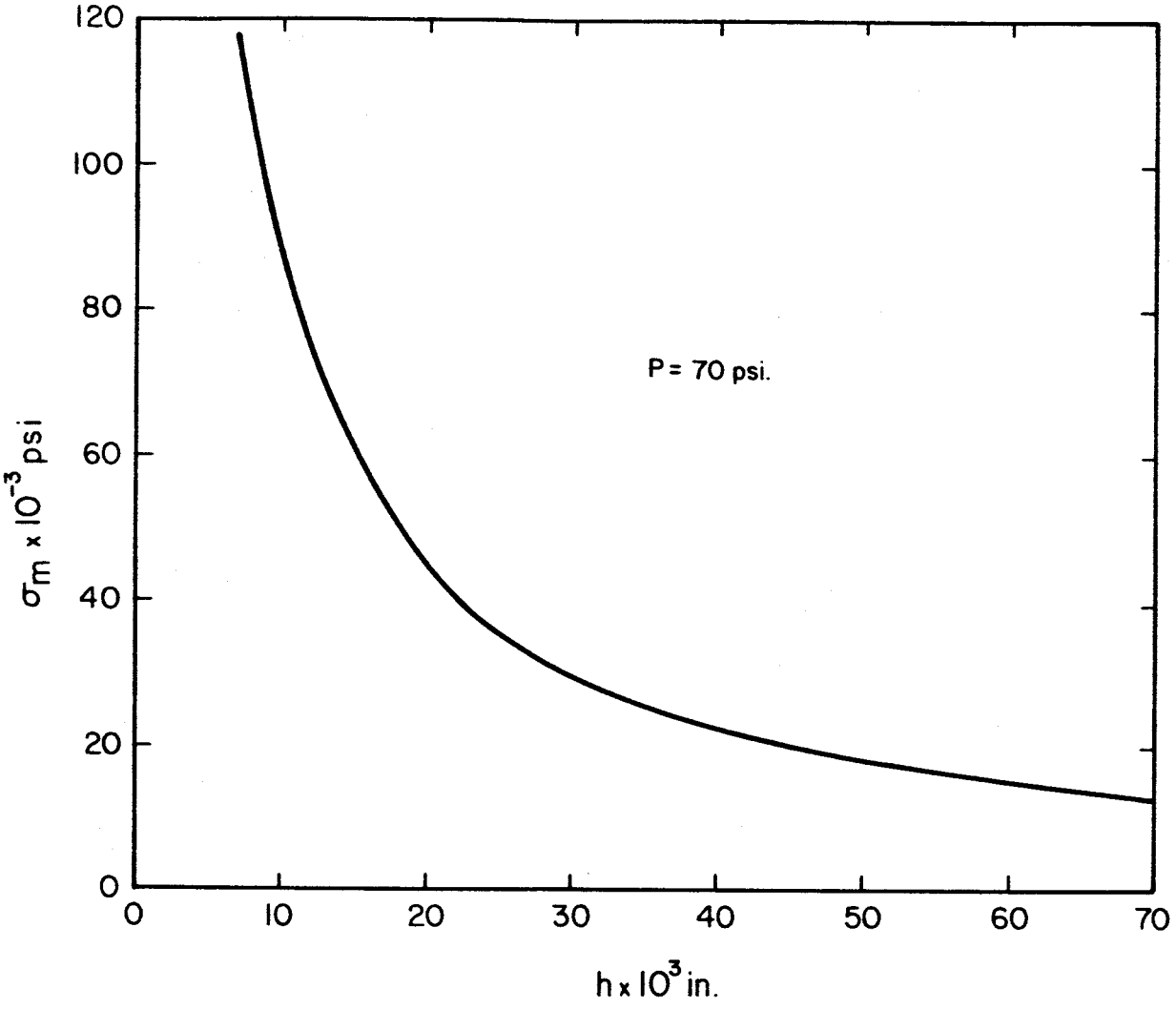

FIG. A-2 MEMBRANE STRESS STATE

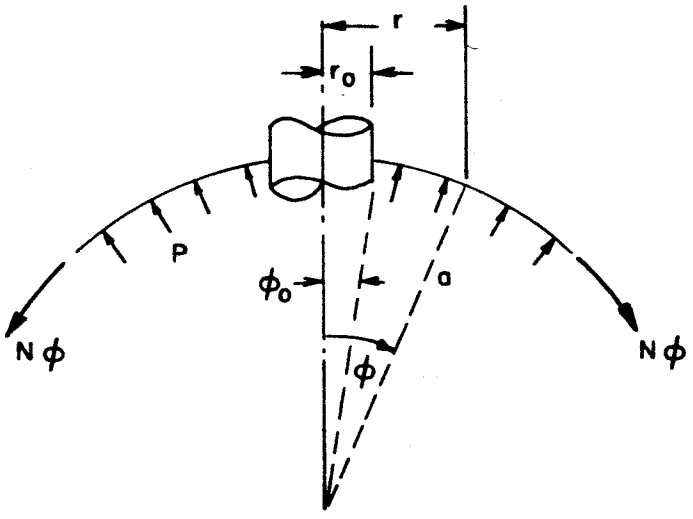

FIG. A-3a CONTAINER BOSS NOMENCLATURE

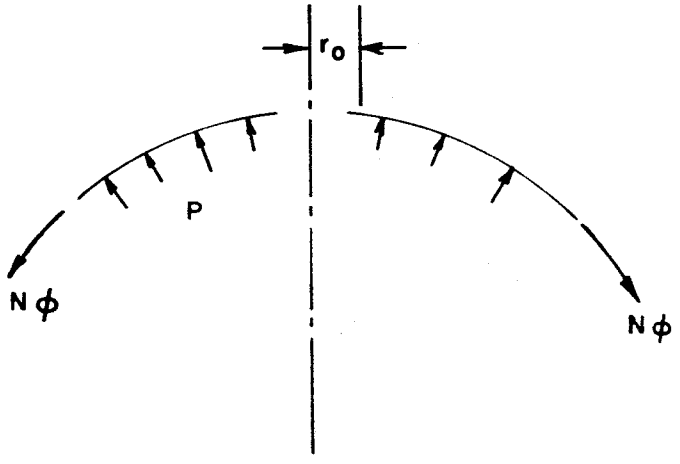

FIG. A-3b CONTAINER BOSS NOMENCLATURE

$$\frac{\sigma_\theta}{\sigma_m} = 1 + \left\{ (1-\nu)\, \Psi_3'(\xi_o) \left[\Psi_4(\xi) - \frac{\Psi_3(\xi)}{\xi} + \frac{3}{\sqrt{3(1-\nu^2)}} \left(\frac{1-\nu}{\xi} \Psi_4'(\xi) - \nu\, \Psi_3(\xi) \right) \right] \right.$$

$$\left. - (1-\nu)\, \Psi_4'(\xi_o) \left[\Psi_3(\xi) + \frac{\Psi_4'(\xi)}{\xi} + \frac{3}{3(1-\nu^2)} \left(\frac{1-\nu}{\xi} \Psi_3'(\xi) + \nu\, \Psi_4(\xi) \right) \right] \right\} \quad (3)$$

$$\left\{ \Psi_3(\xi_o)\, \Psi_4'(\xi_o) - \Psi_4(\xi)\, \Psi_3'(\xi_o) + \frac{1+\nu}{\xi_o} \left(\Psi_3'^2(\xi_o) + \Psi_4'^2(\xi_o) \right) \right\}^{-1}$$

(Note: $\frac{\sigma\phi}{\sigma m} \to \frac{2}{1+\nu}$ as $a \to \infty$; $\frac{\sigma_\theta}{\sigma_m} \to \frac{2\nu}{1+\nu}$ as $a \to \infty$)

In the above equations σ_m denotes the previous membrane stress (Pa/2h), Ψ_i are Schleicher functions (Ref. 2), $(\,)'$ denotes d/dξ, $\xi = 1.82\, r/\sqrt{ah}$ ($\nu = 0.3$ has been assumed), $\xi_o = 1.82\, r_o/\sqrt{ah}$, r_o = hole radius, and r = distance from hole centerline. Equations 2 and 3 are numerically illustrated in Figs. A-4a and A-4b. These data indicate a stress concentration factor of approximately $\frac{\sigma_\phi}{\sigma_m} = 2$ to 2.5 exists for a = 25.5 in. and h = 30×10^{-3} to 60×10^{-3} in. r_o = 1 to 2 in. This concentration (in meridional stress) is the direct result of local bending near the insert.

Now let us assume the intersecting body possesses zero flexibility. The mathematical equivalent of this is a hole. Since ro << **a**, the stress concentration will be approximately that of a plate (infinite) with a hole subjected to bitension. For such a case the stress concentration factor is $\sigma_\phi / \sigma_m = \sigma_\theta / \sigma_m = 2$ at the edge of the hole.

The above limit cases indicate the magnitude of the stress concentrations one can expect for a shell of constant thickness. They can be eliminated to a certain degree by an appropriate flaring of the connecting body and varying the sphere's thickness near the flange area.

Temperature Induced Stresses: As mentioned previously, these arise from two sources: (1) temperature gradients in the ϕ direction, and (2) temperature gradients through the shell wall. Their effects can be considered separately and the results can be superimposed to determine the total stress field.

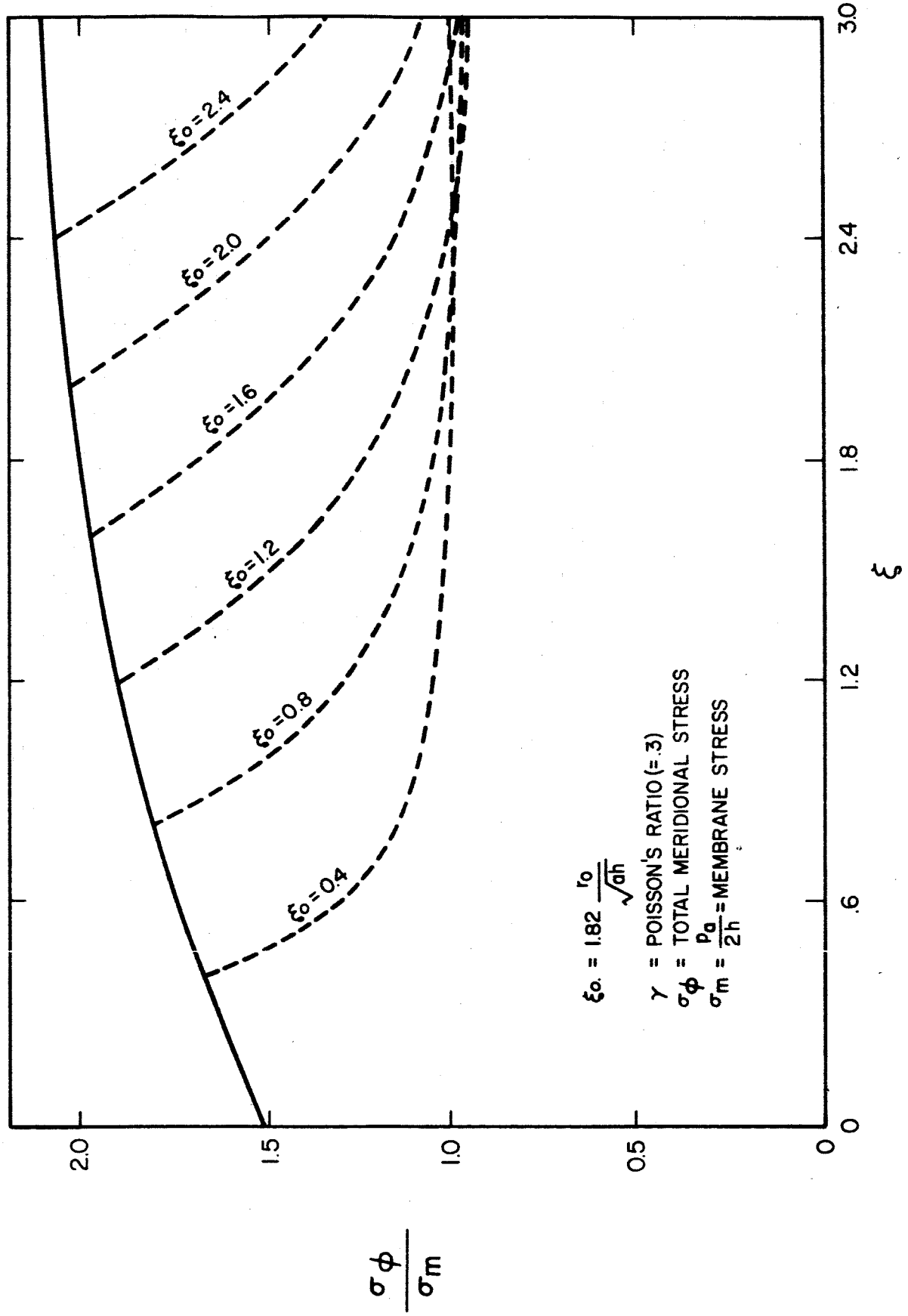

FIG. A-4a MAXIMUM TOTAL MERIDIONAL STRESSES (MEMBRANE PLUS BENDING) IN A PRESSURIZED SPHERICAL SHELL CONTAINING A RIGID INSERT

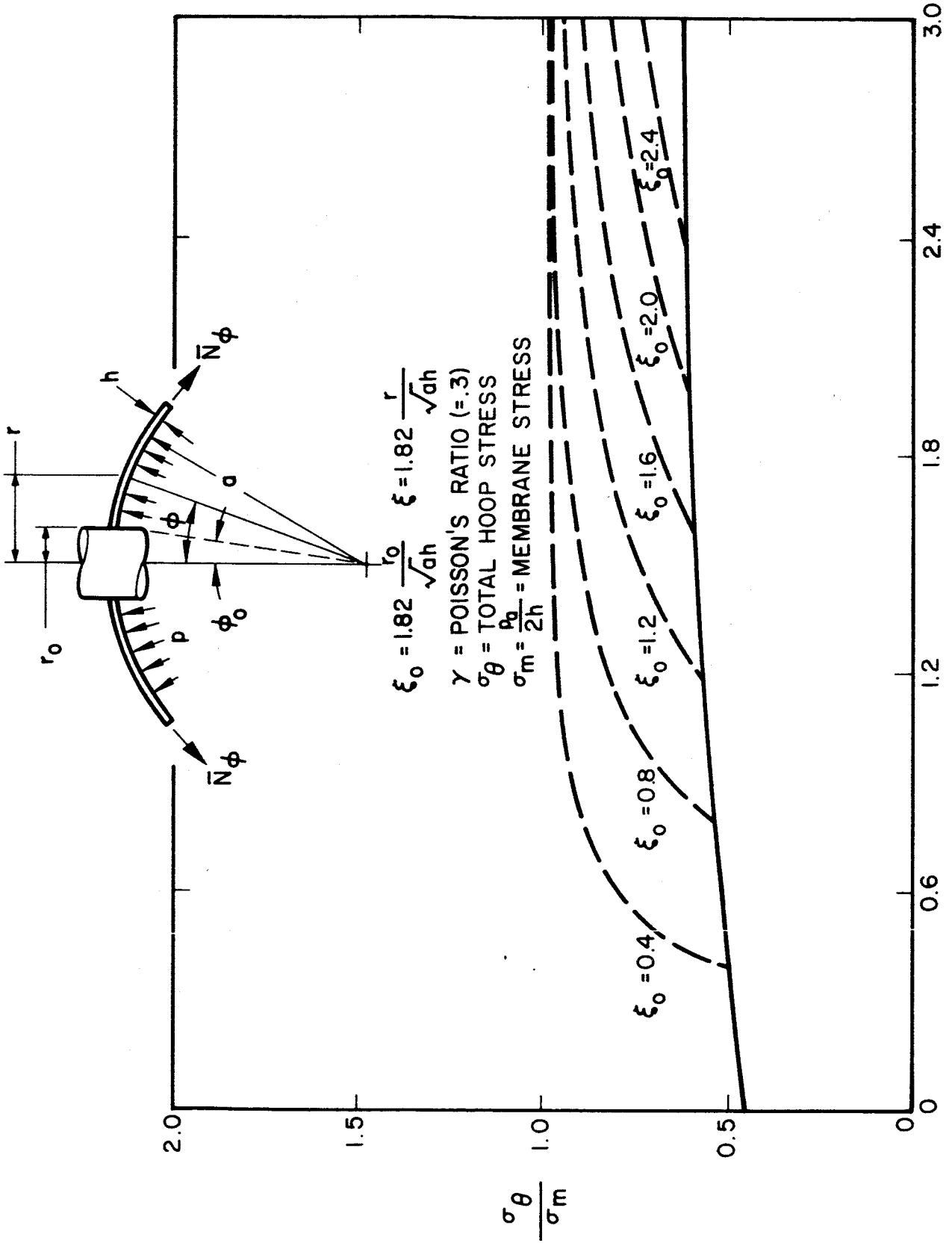

FIG. A-4b MAXIMUM TOTAL HOOP STRESSES (MEMBRANE PLUS BENDING) IN A PRESSURIZED SPHERICAL SHELL CONTAINING A RIGID INSERT

A representative estimate of the stresses induced by item 1 can be obtained by considering the tank at the one-half-full mark.

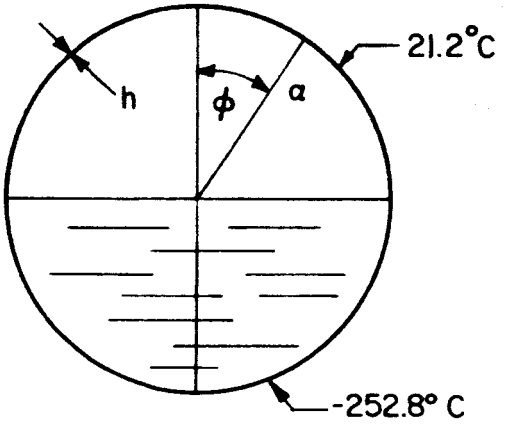

If the cold and warm hemispheres are cut apart along the equator, there will exist a gap = $a\alpha T$ (no thermal stresses exist when cut).

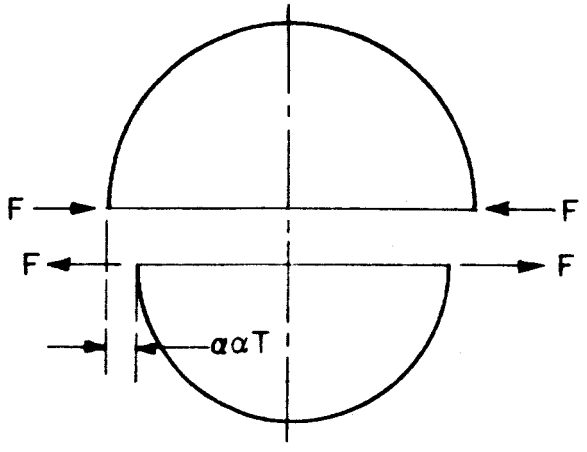

Here α = coefficient of thermal expansion and T = average wall temperature. To close the gap radial forces, F, must be applied, bending the upper shell inward and the lower outward by the same amount = 1/2 $a\alpha T$. This produces a hoop strain of $\epsilon\theta = \pm 1/2\ \alpha T$. From the symmetry the rotation will be the same at both edges so that the tangent to the meridian will be continuous without the application of moments. After some calculation one finds:

$$(\sigma_\theta)_{T_{max}} = \frac{(N_\theta)_T}{h} \pm \frac{6(M_\theta)_T}{h^2}$$

$$(\sigma_\phi)_{T_{max}} = \frac{(N_\phi)_T}{h} \pm \frac{6(M_\phi)_T}{h^2} \qquad (4)$$

where the subscript "T" indicates thermal stress only, i.e., the membrane stress due to pressure has not been included. In Eq. 4 N_θ, N_ϕ, M_θ, M_ϕ are given by

$$(N_\theta)_T = -\frac{Eh\alpha T}{2} e^{-Hw} \sin(Hw - \pi/2)$$

$$(N_\phi)_T = -Q_\phi \cot\phi$$

$$Q_\phi = \frac{Eh\alpha T}{4H}\sqrt{2}\, e^{-Hw} \sin(Hw - \pi/4) \qquad (5)$$

$$M_\phi = \frac{aE\alpha Th}{4H^2} e^{-Hw} \sin(Hw)$$

$$M_\theta = \nu M_\phi$$

where $H^4 = 3(1-\nu^2)\, a^2/h^2$. Note that since N_θ, $N_\phi \sim h$ and M_θ, $M_\phi \sim h^2$ the maximum amplitude of the thermal stresses, Eq. 4, are independent of wall thickness. These stresses are illustrated numerically in Fig. A-5 for a = 25.5 in., h = 34 x 10^{-3} in., E = 30 x 10^6 psi, $\alpha = 10^{-5}$ in/in/°C and $\nu = 0.3$, T = 21.2°C + 252.8°C = 274°C. An increase in shell thickness will stretch the vertical scale (smooth out the distribution) but will not affect the horizontal scale (amplitude). Note that the amplitudes of the stresses are directly proportional to EαT. For h = 34 x 10^{-3} in. the zone of influence of the above stresses is about $\phi = 4^\circ$, hence they are quite confined.

Let us estimate the effect of an initial thermal gradient through the tank thickness by assuming the temperatures at the outer and inner surfaces of a spherical shell are constant in the area already filled with fluid, but that there exists a linear variation of temperature in the radial direction. If ΔT is the difference in the temperatures of the outer and inner surfaces, the stresses some distance from the gas-fluid interface are given approximately by:

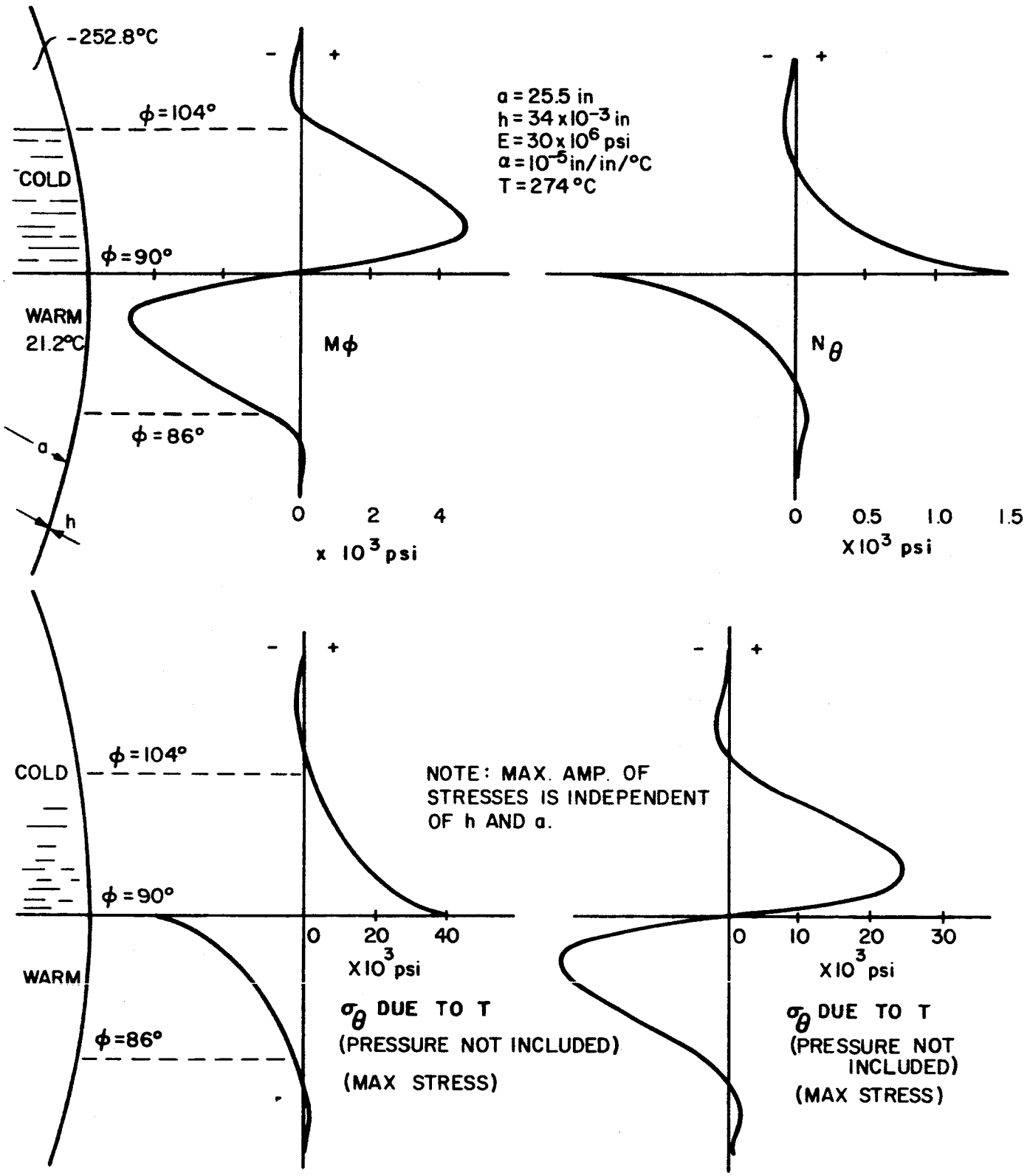

FIG. A-5 THERMAL STRESSES DUE TO GRADIENT IN ϕ DIRECTION

$$(\sigma_\phi)_{\Delta T}{}_{max} = (\sigma_\theta)_{\Delta T}{}_{max} = \alpha \Delta T E/2(1-\nu) \quad (6)$$

Assuming $E = 30 \times 10^6$ psi, $\alpha = 10^{-5}$ in/in/^oC, $\Delta T = 274^oC$, $\nu = 0.3$, one obtains

$$(\sigma_\phi)_{max} = (\sigma_\theta)_{max} = 58{,}700 \text{ psi.}$$

Note again that the magnitude of the stress is independent of thickness and is directly proportional to $E\alpha\Delta T$. Equation 6 is illustrated for various values of ΔT, α and E in Fig. A-6.

4. SUMMARY

For design purposes, Figs. A-2, A-5 and A-6 represent expected membrane and maximum temperature induced stress levels. The total maximum stress in any given case is obtained by all three types of stresses shown. In the area of the flanges, a stress concentration factor of 2.5 should be assumed for a constant thickness shell (the factor 2.5 is based on the membrane stress). An appropriate flaring of the inlet (exhaust) pipes and an increase in shell thickness near the flange area will significantly reduce this factor.

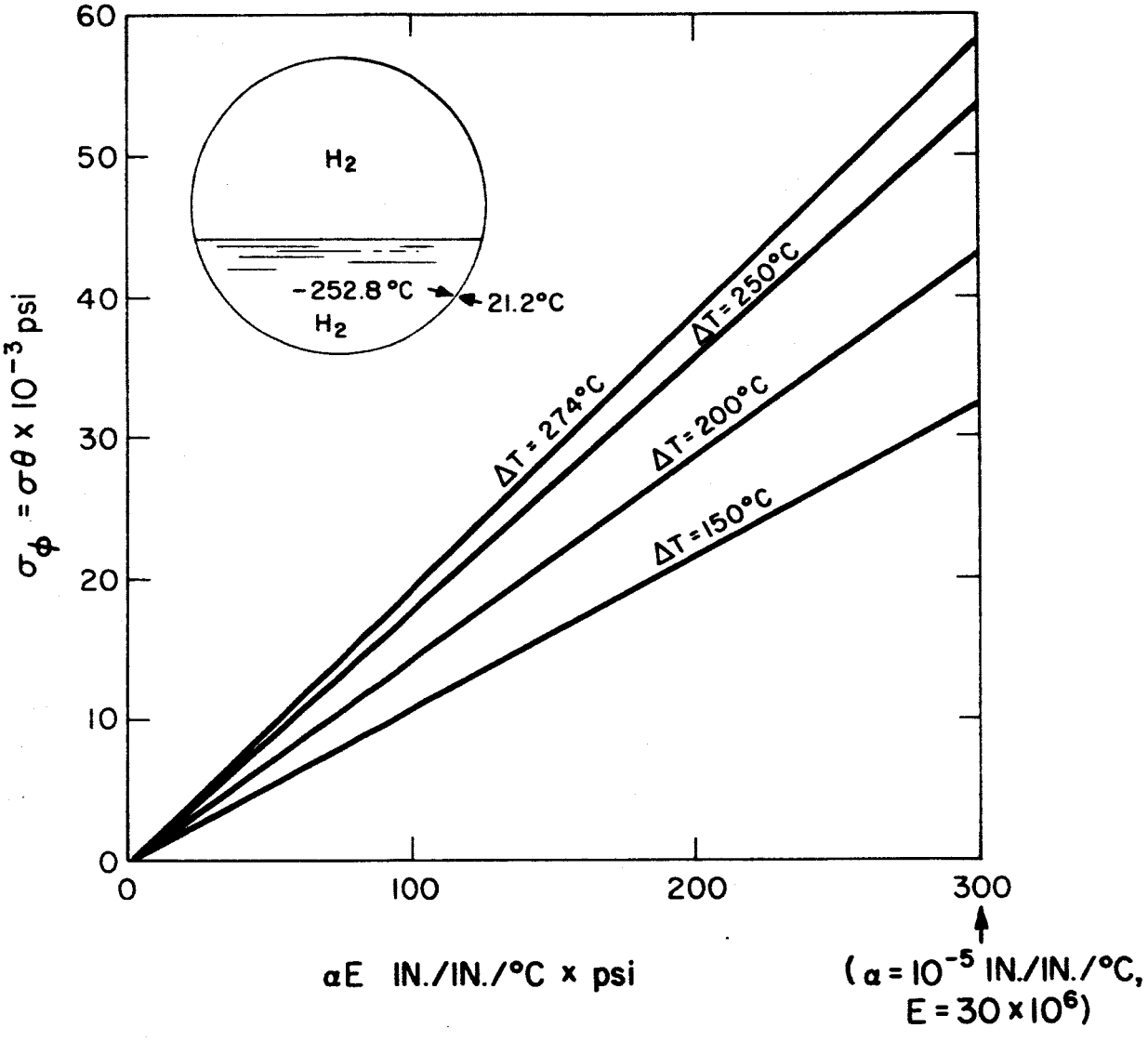

FIG. A-6 INITIAL THERMAL STRESS IN FILLED REGION DUE TO RADIAL TEMPERATURE DISTRIBUTION

REFERENCES

APPENDIX

1. L. B. Greszczuk, "Stress Distribution in a Pressurized Spherical Shell Containing a Rigid Insert at the Apex," Douglas Aircraft Rep. No. 1289, September 28, 1961

2. S. Timoshenko, Theory of Plates and Shells, McGraw-Hill, New York, 1940, pp. 418-420, 450-473

3. W. Flugge, Stresses in Shells, Springer-Verlag, Berlin, 1960

4. P. P. Bijlaard, "Computation of Stresses from Local Loads in Spherical Pressure Vessels or Pressure Vessel Heads, "Welding Research Council Bulletin 34," 1957, p. 8

APPENDIX B

DERIVATION OF ANODE PACK DESIGN EQUATION

BY R. N. HANSON

1. INTRODUCTION

The vessel fabricated during this program rotated in the electroforming bath about a horizontal center shaft. Half of the vessel was submerged in the electroforming solution. It was required that the nickel anodes be placed in the electroforming solution below the rotating mandrel. As the vessel was to be of constant wall thickness the main anode pack had to be designed to maintain a constant current density on the area of the mandrel rotating above it. This could not be accomplished with a constant width anode basket; therefore the following equation was developed to define the required width of the anode pack at any location under the mandrel.

2. DEVELOPMENT OF WIDTH EQUATION

The geometry of the electroforming setup with definition of symbols is shown in Fig. B-1.

Masks are placed on the sides, ends and rear surface of the anode pack so that the only current flow is directed from the normal to the surface of the anode pack along the radius to the center of the sphere.

Assuming that the width of the anode pack is small compared to the diameter of the sphere, the surface area of the anode pack at any angle θ, is given by:

$$dA_{anode} = W_{\theta} (R+h) \, d\theta \qquad (1)$$

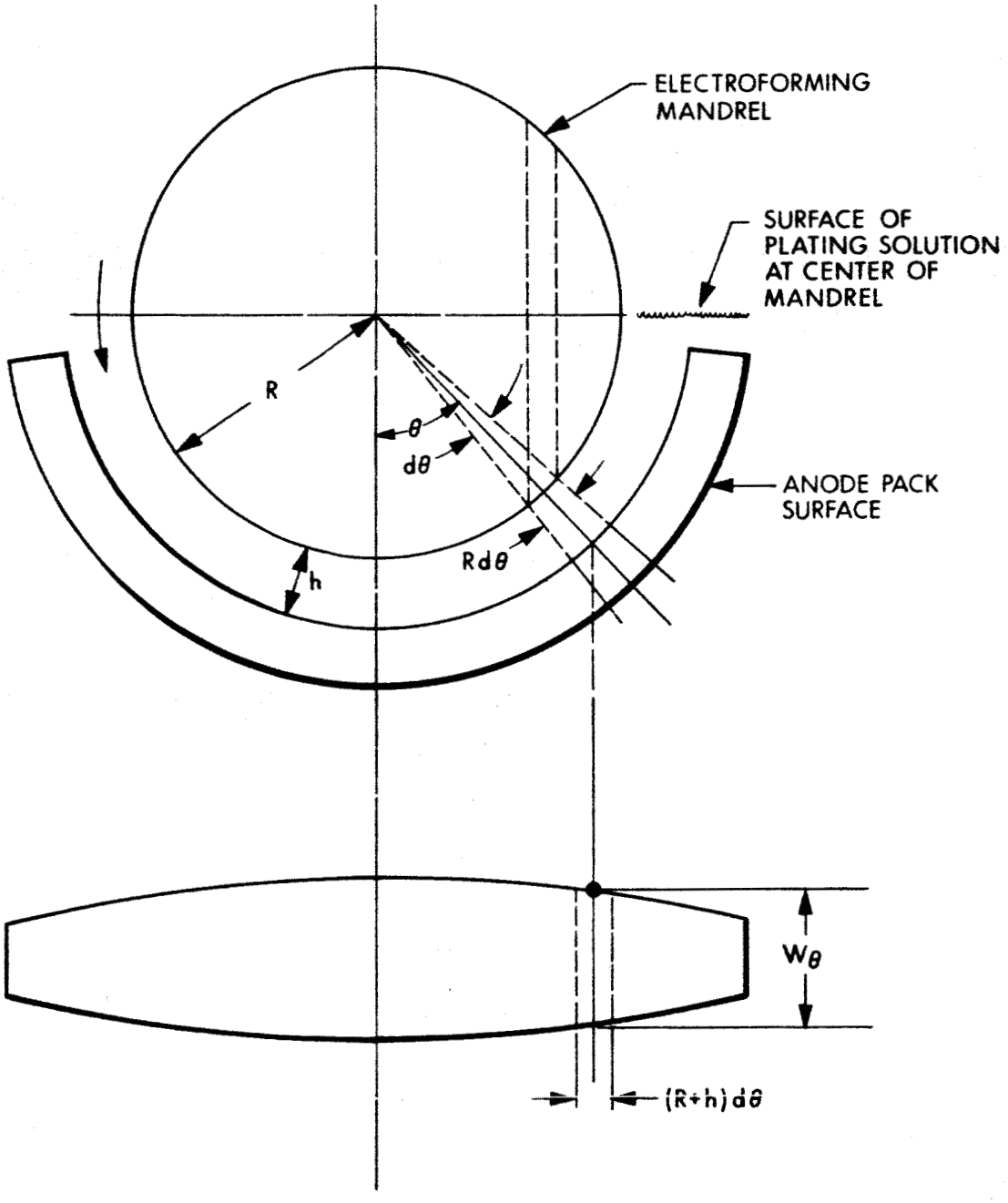

FIG. B-1 ELECTROFORMING BATH GEOMETRY AND SYMBOLS

Where:

W_θ = width of anode pack at any angle θ, in inches
R = radius of mandrel, in inches
h = distance between surface of mandrel and anode pack, in inches

Because the mandrel is rotating, the corresponding area on the surface of the mandrel is given by:

$$dA_{mandrel} = 2\pi R^2 \cos \theta d\theta \qquad (2)$$

For uniform wall thickness the ratio of the mandrel surface area to the anode pack surface area must be constant, giving

$$\frac{dA_{mandrel}}{dA_{anode}} = K \qquad (3)$$

Substituting equations (1) and (2) in (3) the width of the anode pack at any angle θ is given by:

$$W_\theta = \frac{2\pi R^2 \cos \theta}{K (R + h)}$$